Electronic Supporting Information

What Controls the Magnetic Anisotropy in Heptacoordinate High-Spin Cobalt(II) Complexes? A Theoretical Perspective

Peter Comba[1]*, Gopalan Rajaraman[2]*, Arup Sarkar[2] and Gunasekaran Velmurugan[1]

[1]Heidelberg University, Institute of Inorganic Chemistry and Interdisciplinary Center for Scientific Computing, Im Neuenheimer Feld 270, 69120 Heidelberg, Germany. E-mail: peter.comba@aci.uni-heidelberg.de

[2]Department of Chemistry, Indian Institute of Technology Bombay, Powai, Mumbai, 400076, India. E-mail: rajaraman@chem.iitb.ac.in

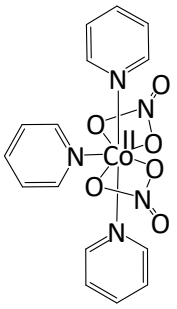

$[Co(py)_3(NO_3)_2]$ (**1**)

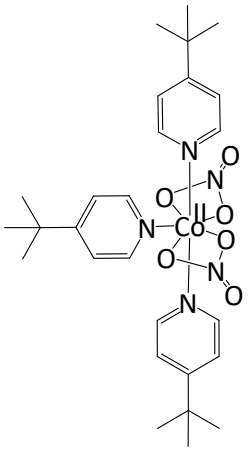

$[Co(tbp)_3(NO_3)_2]$ (**2**)

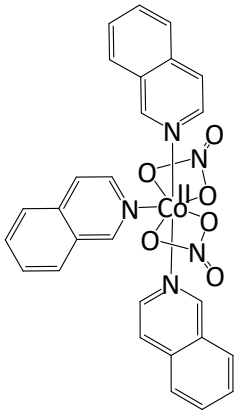

$[Co(isq)_3(NO_3)_2]$ (**3**)

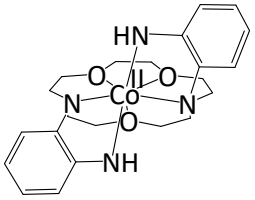

$[Co(L_1)]^{2+}$ (**4**)

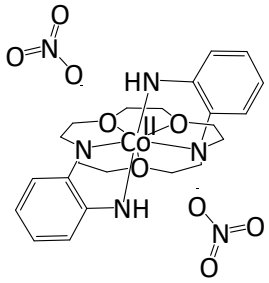

$[Co(L_1)].2NO_3$ (**5**)

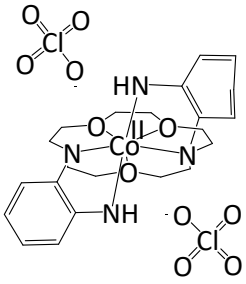

$[Co(L_1)].2ClO_4$ (**6**)

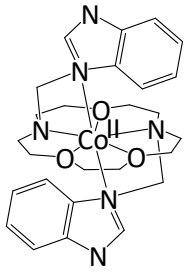

$[Co(L_2)]^{2+}$ (**7**)

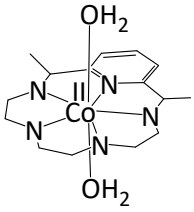

$[Co(L_3)(H_2O)_2]^{2+}$ (**8**)

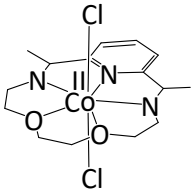

$[Co(L_4)Cl_2]$ (**9**)

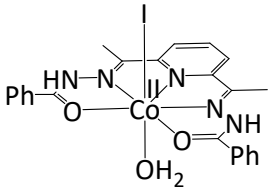

$[Co(L_5H_2)I(H_2O)]$(**10**)

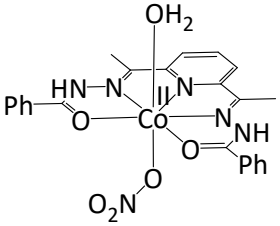

$[Co(L_5H_2)(H_2O)(NO_3)]$(**11**)

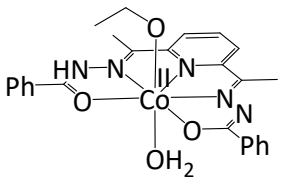

$[Co(L_5H)(H_2O)(EtOH)]^{+}$(**12**)

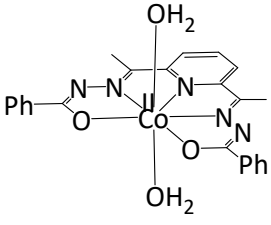

$[Co(L_5)(H_2O)]$ (**13**)

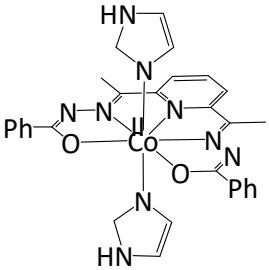

$[Co(L_5)(im)_2]$ (**14**)

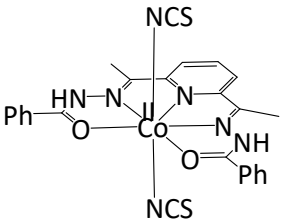

$[Co(L_5H_2)(NCS)_2]$ (**15**)

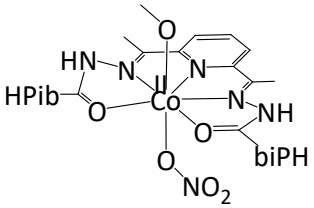

$[Co(NO_3)(EtOH)]^{+}$(**16**)

Scheme S1. Structural formula of the chosen heptacoordinate high-spin Co^{II} complexes;

Table S1. SHAPE parameter of the investigated seven coordinate complexes.

Complex	JETPY (C_{3v})	JPBPY (D_{5h})	CTPR (C_{2v})	COC (C_{3v})	PBPY (D_{5h})	HPY (C_{6v})	HP (D_{7h})
$[Co(py)_3(NO_3)_2]$ (**1**)	23.24	4.37	6.31	8.32	1.45	23.94	32.49
$[Co(tbp)_3(NO_3)_2]$ (**2**)	22.35	4.52	6.79	8.22	1.41	24.56	33.24
$[Co(isq)_3(NO_3)_2]$ (**3**)	22.28	4.69	6.59	8.25	1.54	22.96	32.27
$[Co(L_1)]^{2+}$ (**4**)	22.10	3.80	4.92	6.42	0.55	25.48	33.65
$[Co(L_1)]\cdot 2NO_3$ (**5**)	22.10	3.80	4.92	6.42	0.55	25.48	33.65
$[Co(L_1)]\cdot 2ClO_4$ (**6**)	22.10	3.80	4.92	6.42	0.55	25.48	33.65
$[Co(L_2)]^{2+}$ (**7**)	19.74	3.46	5.24	6.76	1.10	23.42	28.81
$[Co(L_3)(H_2O)_2]^{2+}$ (**8**)	22.68	3.50	4.92	6.46	0.29	24.66	33.80
$[Co(L_4)Cl_2]$ (**9**)	23.94	5.74	5.07	6.58	0.50	25.38	35.64
$[Co(L_5H_2)I(H_2O)]$ (**10**)	24.61	6.52	6.89	8.48	1.01	25.45	34.34
$[Co(L_5H_2)(H_2O)(NO_3)]$ (**11**)	22.92	3.58	5.08	6.59	0.42	23.94	32.34
$[Co(L_5H)(H_2O)(EtOH)]^{+}$ (**12**)	23.95	3.35	5.89	7.67	0.13	25.26	33.85
$[Co(L_5)(H_2O)]$ (**13**)	23.77	3.14	5.21	6.57	0.34	23.17	33.44
$[Co(L_5)(im)_2]$ (**14**)	22.49	3.21	5.99	7.75	0.40	23.01	33.77
$[Co(L_5H_2)(NCS)_2]$ (**15**)	23.58	2.93	5.59	7.33	0.25	24.45	33.69
$[Co(NO_3)(EtOH)]^{+}$ (**16**)	24.00	3.38	5.64	7.36	0.20	24.73	32.87

JETPY = Johnson elongated triangular pyramid, JPBPY = Johnson pentagonal bipyramid, CTPR = capped trigonal prism, COC = capped octahedron, PBPY = pentagonal bipyramid, HPY = hexagonal pyramid, HP = heptagon.

Complexes	**CAS(7,5)SCF/NEVPT2**		**CAS(7,10)SCF/NEVPT2**	
	D **(cm^{-1})**	***E/D***	***D*** **(cm^{-1})**	***E/D***
1	40.78	0.07	41.27	0.07
2	61.74	0.26	62.15	0.25
3	40.83	0.12	41.98	0.11
4	31.34	0.14	33.08	0.13
5	31.35	0.14	33.09	0.13
6	31.35	0.14	33.09	0.13
7	30.49	0.12	32.33	0.12
8	35.15	0.02	35.21	0.02
9	47.30	0.04	47.14	0.04
10	36.97	0.03	37.84	0.03
11	35.50	0.07	36.08	0.07
12	37.51	0.01	37.96	0.01
13	34.35	0.06	34.74	0.06
14	35.00	0.06	35.34	0.06
15	38.07	0.05	38.77	0.05
16	38.21	0.01	38.40	0.02

Table S2: Comparison of ZFS parameters obtained from different active space calculations:

Table S3. Ab initio ligand field (AILFT) parameters with CAS(7,5) active space fitted to NEVPT2 energies.

Complex	Orbital energies (cm^{-1})					B (cm^{-1})	C/B	ζ (cm^{-1})
	d_{xz}	d_{yz}	d_{xy}	$d_{x^2-y^2}$	d_{z^2}			
$[Co(py)_3(NO_3)_2]$ (**1**)	0	280	2537	4598	8846	1000	3.84	523
$[Co(tbp)_3(NO_3)_2]$ (**2**)	0	723	1403	6260	8735	1003	3.83	520
$[Co(isq)_3(NO_3)_2]$ (**3**)	0	498	1841	5821	9080	1002	3.83	520
$[Co(L_1)]^{2+}$ (**4**)	0	293	4066	4273	8307	1001	3.85	520
$[Co(L_1)]\cdot 2NO_3$ (**5**)	0	372	4061	4308	8310	1001	3.85	520
$[Co(L_1)]\cdot 2ClO_4$ (**6**)	0	372	4097	4335	8286	1001	3.85	520
$[Co(L_2)]^{2+}$ (**7**)	0	707	2600	3486	8399	1001	3.86	521
$[Co(L_3)(H_2O)_2]^{2+}$ (**8**)	0	353	5866	6224	6492	1006	3.84	520
$[Co(L_4)Cl_2]$ (**9**)	0	53	2102	5267	6348	995	3.90	518
$[Co(L_5H_2)I(H_2O)]$ (**10**)	0	144	4277	5254	6152	1000	3.89	518
$[Co(L_5H_2)(H_2O)(NO_3)]$ (**11**)	0	531	4614	4828	7225	1003	3.87	521
$[Co(L_5H)(H_2O)(EtOH)]^{+}$ (**12**)	0	781	4761	6526	6845	1006	3.87	521
$[Co(L_5)(H_2O)]$ (**13**)	0	66	5202	5570	7169	1004	3.85	521
$[Co(L_5)(im)_2]$ (**14**)	0	232	4683	4854	8958	993	3.84	520
$[Co(L_5H_2)(NCS)_2]$ (**15**)	0	200	2704	3703	8707	992	3.86	521
$[Co(NO_3)(EtOH)]^{+}$ (**16**)	0	348	4383	4626	7418	1000	3.88	521

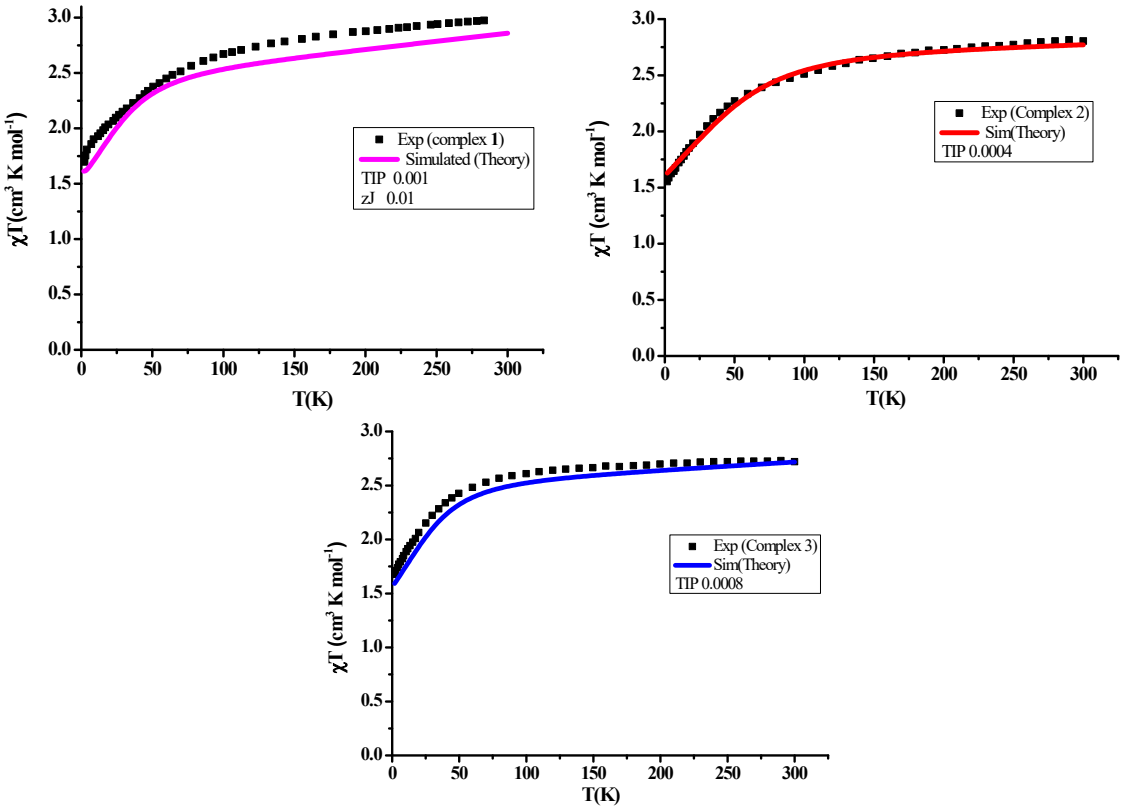

Figure S1: Comparison of the χT vs T experimental plots of complex **1** (top left), **2** (top right) and complex **3** (bottom) versus NEVPT2 simulated ones.[2]

,

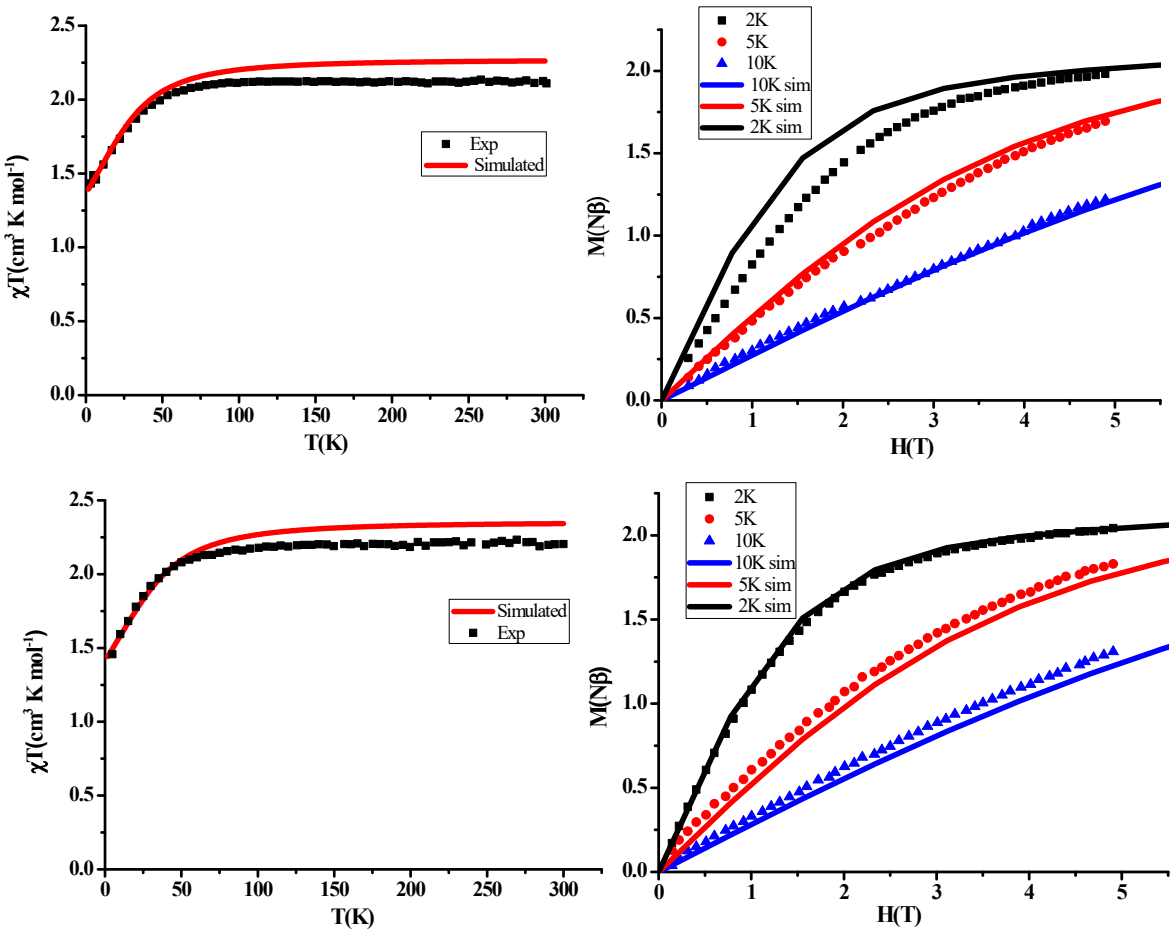

Figure S2. Comparison of the χT vs T and M vs H plots for complexes **13**[1] (top) and **15**[1] (bottom) with the simulations obtained from NEVPT2 level of theory.

Table S4. Comparison of the calculated parameter for the magnetic anisotropy of $[Co(py)_3(NO_3)_2]$ (**1**) at different levels of theory.

Calculated parameters	CASSCF	NEVPT2	Experimental values
D (cm^{-1})	49.46	40.78	68.7
E/D	0.08	0.07	0.07
g_z	1.99	2.00	-
g_y	2.44	2.34	-
g_x	2.52	2.40	-
g_{iso}	2.32	2.25	2.43

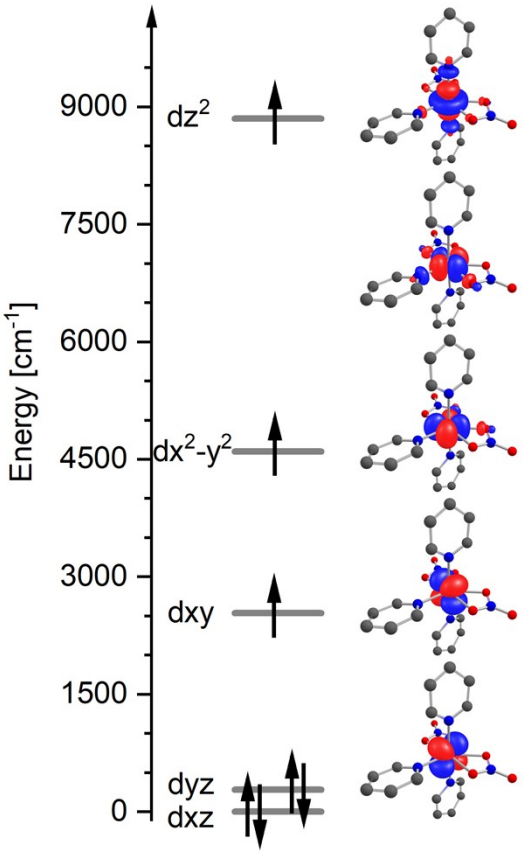

Figure S3. AILFT orbital energy diagram for $[Co(py)_3(NO_3)_2]$ (**1**).

Table S5. Details of the major contributing excitations that lead to the D- and E-values (NEVPT2 level of theory) calculated for $[Co(py)_3(NO_3)_2]$ (**1**).

NEVPT2 excited states	NEVPT2 energy (cm^{-1})	%	Major electronic configuration					Contribution to D (cm^{-1})	Contribution to E (cm^{-1})
			d_{xz} (0)	d_{yz} (280)	d_{xy} (2536)	$d_{x^2-y^2}$ (4598)	d_{z^2} (8846)		
$^4A_2'$	0	87	2	2	1	1	1	0	0
		11	1	1	2	2	1		
$^4E_2''$	2423	81	2	1	2	1	1	5.02	-5.49
		15	1	2	1	2	1		
	2870	77	1	2	2	1	1	3.96	3.96
		19	2	1	1	2	1		
$^4E_1''$	4970	64	2	1	1	2	1	15.29	15.29
		27	2	1	1	1	2		
	6302	70	1	2	1	2	1	10.65	-10.80
		23	1	2	1	1	2		
$^2A_1'$	16894	90	2	2	1	1	1	4.94	0.02
$^2A_1'$	21629	73	1	2	1	1	2	7.97	0.01
		14	1	2	1	2	1		
		13	2	1	2	1	1		

Table S6. Computed NEVPT2 transition energies and state-wise contribution to the axial and rhombic ZFS parameters of $[Co(py)_3(NO_3)_2]$ (**1**).

NEVPT2 excited states	Multiplicity	NEVPT2 energy (cm^{-1})	Contribution to D (cm^{-1})	Contribution to E (cm^{-1})
0	4	0	0.00	0.00
1	4	2423	5.02	-5.49
2	4	2870	3.96	3.96
3	4	4970	15.29	15.29
4	4	6302	10.65	-10.83
5	4	12118	0.02	0.02
6	2	12457	0.17	0.04
7	4	14831	0.00	0.00
8	2	14876	0.00	0.00
9	2	16894	4.94	0.02
10	2	18560	0.00	0.00
11	2	20104	-0.65	0.70
12	2	20661	-1.27	-1.27
13	2	21201	-0.83	0.86
14	2	21226	-0.40	-0.40
15	4	21372	0.01	0.01
16	2	21629	7.97	0.01
17	4	22049	0.14	-0.14
18	2	22477	0.00	0.00
19	4	22707	0.10	0.10
20	2	22827	0.01	0.01
21	2	23447	0.00	0.00
22	2	26976	-0.06	-0.06
23	2	27146	-0.07	0.07
24	2	29050	-0.12	0.15
25	2	29512	-0.07	-0.07
26	2	29934	-0.06	-0.06
27	2	31244	0.36	0.02
28	2	31818	0.03	0.09
29	2	31980	-0.07	-0.07
30	2	32029	-0.03	-0.03
31	2	32449	0.13	0.02
32	2	33076	0.99	0.00
33	2	33143	0.00	0.00
34	2	33640	-0.02	-0.02

35	2	33707	0.01	0.04
36	2	35140	-0.54	-0.54
37	2	35323	-0.68	0.68
38	2	42265	-0.22	-0.22
39	2	42932	-0.23	0.24
40	2	43481	0.00	0.00
41	2	43674	0.00	0.00
42	2	43820	-0.05	-0.05
43	2	43997	0.00	0.00
44	2	44638	0.00	0.00
45	2	63982	0.16	0.00
46	2	64048	0.00	0.00
47	2	64721	0.04	0.00
48	2	65219	0.00	0.00
49	2	65431	0.01	0.00

Table S7. Comparison of the calculated parameter for the magnetic anisotropy of $[Co(tbp)_3(NO_3)_2]$ (**2**) at different levels of theory.

Calculated parameters	CASSCF	NEVPT2	Experimental values
D (cm^{-1})	78.40	61.74	35.8
E/D	0.25	0.26	0.00
g_z	1.95	1.97	1.98
g_y	2.40	2.35	2.21
g_x	2.85	2.72	2.21
g_{iso}	2.4	2.35	2.13

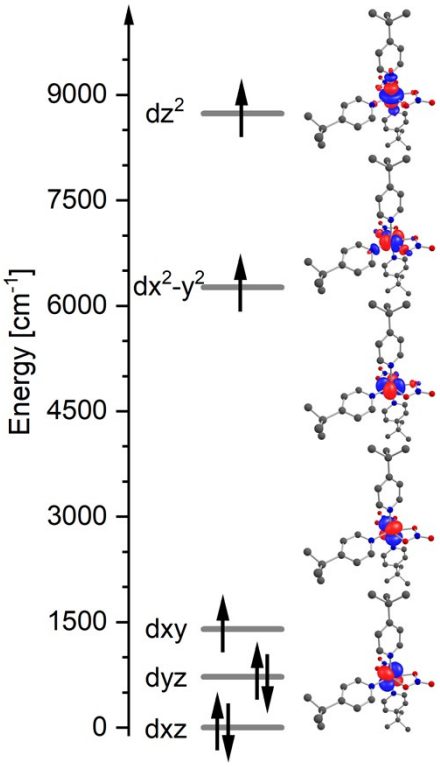

Figure S4. AILFT orbital energy diagram for $[Co(tbp)_3(NO_3)_2]$ (**2**).

Table S8. Details of the major contributing excitations that lead to the D- and E-values (NEVPT2 level of theory) calculated for $[Co(tbp)_3(NO_3)_2]$ (**2**).

NEVPT2 excited states	NEVPT2 energy (cm^{-1})	%	Major electronic configuration					Contribution to D (cm^{-1})	Contribution to E (cm^{-1})
			d_{xz} (0)	d_{yz} (723)	d_{xy} (1403)	$d_{x^2-y^2}$ (6260)	d_{z^2} (8735)		
$^4A_2$	0	83	2	2	1	1	1	0	0
		11	1	1	2	2	1		
$^4B_1$	927	74	2	1	2	1	1	28.68	28.87
		11	1	2	2	1	1		
$^4B_2$	1727	71	1	2	2	1	1	11.34	-11.74
		12	2	1	2	1	1		
$^4B_1$	6774	41	2	1	1	2	1	7.863	5.32
		35	1	2	1	2	1		
		11	1	2	1	1	2		
$^4B_2$	7003	37	1	2	1	2	1	5.21	-5.69
		33	2	1	1	2	1		
		13	2	1	1	1	2		
		12	1	2	1	1	2		
$^2A_1$	13899	82	2	2	2	0	1	6.86	0.07
$^2A_1$	23892	51	2	2	0	2	1	4.88	-0.00
		13	2	0	2	1	2		
		13	0	2	2	1	2		

Table S9. Computed NEVPT2 transition energies and state-wise contribution to the axial and rhombic ZFS parameters of $[Co(tbp)_3(NO_3)_2]$ (**2**).

NEVPT2 excited states	Multiplicity	NEVPT2 energy (cm^{-1})	Contribution to D (cm^{-1})	Contribution to E (cm^{-1})
0	4	0	0.00	0.00
1	4	927	28.68	28.87
2	4	1728	11.34	-11.74
3	4	6775	7.86	5.32
4	4	7004	5.21	-5.69
5	4	10102	0.20	-0.18
6	2	11370	0.14	-0.11
7	2	13899	6.86	0.07
8	4	16019	0.00	0.00
9	2	16703	0.01	0.01
10	2	18543	0.00	0.00
11	2	19074	-1.18	-1.14
12	2	19634	-0.60	0.60
13	2	20301	-0.73	0.04
14	2	20513	-0.42	0.41
15	4	21285	0.07	-0.07
16	4	21537	0.04	-0.04
17	2	22496	0.01	0.00
18	2	22671	0.02	0.00
19	4	23037	0.09	0.09
20	2	23227	0.00	0.00
21	2	23892	4.88	0.00
22	2	27247	-0.26	0.13
23	2	27661	-0.39	-0.18
24	2	27952	0.02	0.08
25	2	28695	-0.02	-0.01
26	2	28850	-0.01	0.00
27	2	30400	-0.02	-0.01
28	2	30731	0.98	0.08
29	2	31578	0.09	-0.05
30	2	32783	0.15	0.06
31	2	33167	-0.11	0.08
32	2	33261	-0.06	-0.07

33	2	34162	0.39	0.00
34	2	34237	0.04	0.03
35	2	34604	-0.32	0.35
36	2	34646	-0.12	0.11
37	2	35486	-0.40	-0.38
38	2	41949	-0.08	0.02
39	2	42588	-0.24	-0.06
40	2	43244	0.00	0.00
41	2	43550	0.00	0.00
42	2	43804	0.00	0.00
43	2	44324	-0.07	0.00
44	2	44779	0.00	0.00
45	2	63788	0.12	0.00
46	2	64012	0.00	0.00
47	2	65039	0.00	0.00
48	2	65104	0.00	0.00
49	2	65750	0.06	0.00

Table S10. Comparison of the calculated parameter for the magnetic anisotropy of $[Co(isq)_3(NO_3)_2]$ (**3**) at different levels of theory.

Calculated parameters	CASSCF	NEVPT2	Experimental values
D (cm^{-1})	52.23	40.8	35.7
E/D	0.14	0.13	0.05
g_z	2.04	2.03	2.21
g_y	2.44	2.35	2.21
g_x	2.60	2.46	2.00
g_{iso}	2.36	2.28	2.14

Table S11. Details of the major contributing excitations that lead to the D- and E-values (NEVPT2 level of theory) calculated for $[Co(isq)_3(NO_3)_2]$ (**3**).

NEVPT2 excited states	NEVPT2 energy (cm^{-1})	%	Major electronic configuration					Contribution to D (cm^{-1})	Contribution to E (cm^{-1})
			d_{xz} (0)	d_{yz} (498)	d_{xy} (1841)	$d_{x^2-y^2}$ (5821)	d_{z^2} (9080)		
$^4A_2$	0	78	2	2	1	1	1	0.00	0.00
		10	1	1	2	2	1		
$^4B_1$	1933	67	1	2	2	1	1	11.97	13.53
		18	1	2	2	1	1		
$^4B_2$	2110	61	2	1	2	1	1	8.65	-8.67
		15	1	2	2	1	1		
$^4B_1$	6353	65	2	1	1	2	1	5.73	8.30
		19	2	1	1	1	2		
		11	1	2	1	2	1		
$^4B_2$	7044	63	1	2	1	2	1	8.03	-8.35
		19	1	2	1	1	2		
$^2A_1$	14913	84	2	2	2	0	1	6.12	-0.25
$^2A_1$	23393	60	2	2	0	2	1	5.74	0.00
		10	2	0	2	1	2		
		78	2	2	1	1	1		

Table S12. Computed NEVPT2 transition energies and state-wise contribution to the axial and rhombic ZFS parameters of $[Co(isq)_3(NO_3)_2]$ (**3**).

NEVPT2 excited states	Multiplicity	NEVPT2 energy (cm^{-1})	Contribution to D (cm^{-1})	Contribution to E (cm^{-1})
0	4	0	0.00	0.00
1	4	1933	11.97	13.53
2	4	2110	8.65	-8.67
3	4	6353	5.73	8.30
4	4	7044	8.03	-8.35
5	4	11379	0.16	0.13
6	2	11539	-0.09	0.25
7	2	14913	6.12	-0.25
8	2	15943	-0.03	-0.01
9	4	16215	0.02	-0.01
10	2	18565	0.00	0.00
11	2	19904	-0.71	0.71
12	2	19928	-1.09	-1.17
13	2	20916	-0.58	-0.07
14	2	21122	-0.54	0.44
15	4	21811	0.01	-0.01
16	4	21910	0.10	-0.10

17	2	22765	0.00	0.01
18	2	22819	0.00	0.00
19	4	23250	0.10	0.10
20	2	23393	5.74	0.00
21	2	23437	0.01	0.00
22	2	27276	-0.22	-0.22
23	2	27763	-0.23	0.21
24	2	28726	-0.12	0.12
25	2	28813	-0.06	-0.09
26	2	29851	0.02	0.00
27	2	31273	-0.05	0.02
28	2	31523	0.75	-0.07
29	2	32187	0.02	0.00
30	2	32744	-0.17	0.19
31	2	33029	0.03	-0.08
32	2	33860	-0.12	-0.12
33	2	34279	0.75	0.00
34	2	34280	-0.14	0.14
35	2	34912	-0.13	0.12
36	2	35362	-0.36	0.35
37	2	36091	-0.37	-0.36
38	2	42278	-0.16	0.01
39	2	42883	-0.21	-0.04
40	2	43814	0.03	0.00
41	2	43898	0.00	0.00
42	2	43959	0.00	0.00
43	2	44502	-0.06	0.00
44	2	45079	0.00	0.00
45	2	64075	0.14	0.00
46	2	64319	0.00	0.00
47	2	65213	0.00	0.00
48	2	65425	0.00	0.00
49	2	65969	0.03	0.00

Table S13. Comparison of the calculated parameter for the magnetic anisotropy of $[Co(L_1)]^{2+}$ (**4**) at different levels of theory.

Calculated parameters	CASSCF	NEVPT2	Experimental values
D (cm^{-1})	37.19	31.34	-
E/D	0.15	0.14	-
g_z	2.05	2.04	-
g_y	2.35	2.27	-
g_x	2.48	2.37	-
g_{iso}	2.29	2.23	-

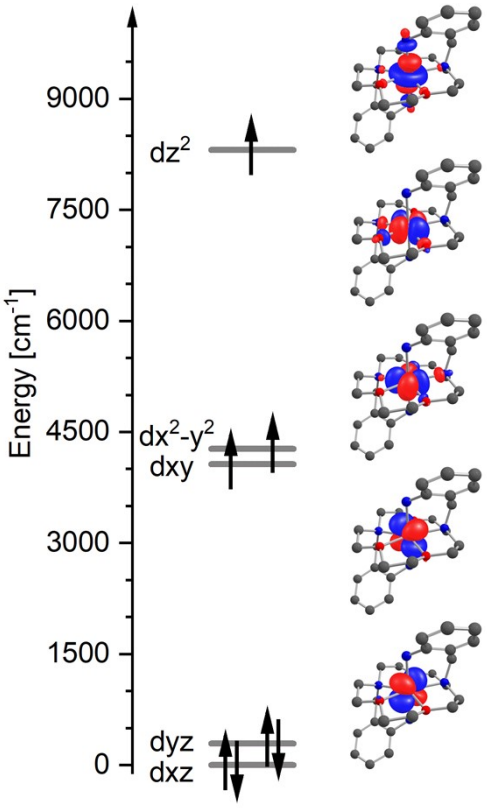

Figure S5. AILFT orbital energy diagram for $[Co(L_1)]^{2+}$ (**4**).

Table S14. Details of the major contributing excitations that lead to the D- and E-values (NEVPT2 level of theory) calculated for $[Co(L_1)]^{2+}$ (**4**).

NEVPT2 excited states	NEVPT2 energy (cm^{-1})	%	Major electronic configuration					Contribution to D (cm^{-1})	Contribution to E (cm^{-1})
			d_{xz} (0)	d_{yz} (293)	d_{xy} (4066)	$d_{x^2-y^2}$ (4273)	d_{z^2} (8307)		
$^4A_2$	0	74	2	2	1	1	1	0.00	0.00
$^4E_2''$	3621	55	1	2	2	1	1	-0.28	2.94
		25	2	1	1	2	1		
	3998	51	1	2	1	2	1	0.35	-0.35
		33	2	1	2	1	1		
$^4E_1''$	5164	32	2	1	1	2	1	13.80	14.30
		26	1	2	1	2	1		
		16	1	2	1	1	2		
		12	2	1	2	1	1		
$^4E_1''$	6176	23	1	2	2	1	1	12.50	12.50
		17	2	1	1	2	1		
		16	2	1	1	1	2		
		16	2	1	2	1	1		
		10	2	2	1	1	1		
$^2A_1'$	20684	17	2	2	2	0	1	8.79	-0.39
		16	1	2	2	1	1		
		14	2	2	0	2	1		
		11	2	1	2	1	1		

Table S15. Computed NEVPT2 transition energies and state-wise contribution to the axial and rhombic ZFS parameters of $[Co(L_1)]^{2+}$ (**4**).

NEVPT2 excited states	Multiplicity	NEVPT2 energy (cm^{-1})	Contribution to D (cm^{-1})	Contribution to E (cm^{-1})
0	4	0	0.00	0.00
1	4	3621	-0.28	2.94
2	4	3998	0.35	-0.35
3	4	5164	13.80	14.30
4	4	6176	12.50	-12.50
5	4	13352	0.05	0.05
6	4	13594	0.04	-0.04
7	2	14672	-0.12	0.12
8	2	14823	0.14	-0.06
9	2	18512	0.14	-0.03
10	2	18557	-0.01	0.01
11	2	20684	8.79	-0.39
12	2	21231	1.69	-0.13
13	2	21305	-0.06	0.06

14	4	21514	0.09	-0.09
15	2	21730	0.09	-1.20
16	2	21966	-1.51	1.51
17	4	22520	0.07	0.07
18	2	22626	0.00	0.00
19	4	22805	0.01	-0.01
20	2	23637	0.00	0.00
21	2	24650	0.00	0.00
22	2	27166	0.02	-0.01
23	2	27309	0.00	0.00
24	2	29646	-0.15	0.15
25	2	29769	-0.22	0.22
26	2	30132	-0.22	-0.23
27	2	30283	-0.03	-0.05
28	2	31472	0.03	-0.03
29	2	31821	-0.03	0.03
30	2	32164	1.28	0.00
31	2	32607	-0.02	-0.02
32	2	32641	-0.01	0.01
33	2	33387	0.00	0.00
34	2	33689	-0.27	0.27
35	2	34032	-0.13	-0.16
36	2	35496	-0.37	-0.37
37	2	35677	-0.42	0.42
38	2	42797	-0.10	-0.11
39	2	42891	-0.07	0.07
40	2	43609	-0.09	-0.11
41	2	43782	-0.11	0.11
42	2	44256	-0.01	0.01
43	2	44364	0.00	0.00
44	2	44513	-0.01	0.01
45	2	64020	0.00	0.00
46	2	64359	0.00	0.00
47	2	64543	0.09	0.00
48	2	65696	-0.01	0.01
49	2	65792	0.10	0.00

Table S16. Comparison of the calculated parameter for the magnetic anisotropy of $[Co(L_1)]\cdot 2NO_3$ (**5**) at different levels of theory.

Calculated parameters	CASSCF	NEVPT2	Experimental values
D (cm^{-1})	37.20	31.35	25.00
E/D	0.15	0.14	0.00
g_z	2.05	2.04	-
g_y	2.36	2.27	-
g_x	2.48	2.37	-
g_{iso}	2.29	2.23	2.22

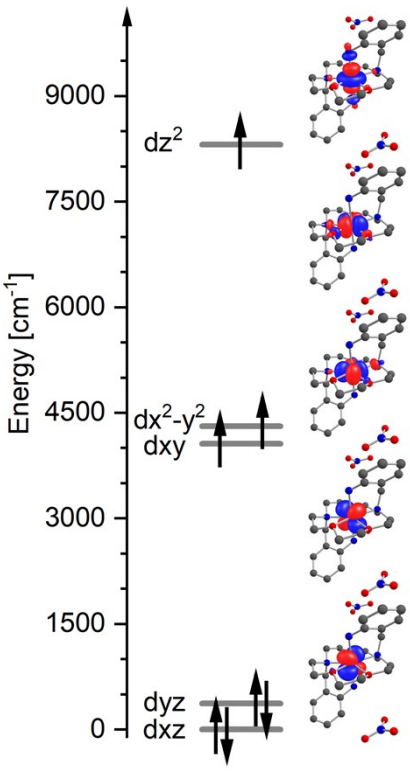

Figure S6. AILFT orbital energy diagram for $[Co(L_1)]\cdot 2NO_3$ (**5**).

Table S17. Details of the major contributing excitations that lead to the D- and E-values (NEVPT2 level of theory) calculated for $[Co(L_1)]\cdot 2NO_3$ (**5**).

NEVPT2 excited states	NEVPT2 energy (cm^{-1})	%	Major electronic configuration					Contribution to D (cm^{-1})	Contribution to E (cm^{-1})
			d_{xz} (0)	d_{yz} (372)	d_{xy} (4061)	$d_{x^2-y^2}$ (4335)	d_{z^2} (8399)		
0	0	78	2	2	1	1	1	0.00	0.00
1	3575	56	1	2	2	1	1	-0.16	3.03
		28	2	1	1	2	1		
2	3965	55	1	2	1	2	1	0.37	-0.38
		34	2	1	2	1	1		
3	5186	32	2	1	1	2	1	13.65	14.12
		23	1	2	1	2	1		
		16	1	2	1	1	2		
		12	2	1	2	1	1		
4	6116	27	1	2	2	1	1	12.62	-12.61
		19	2	1	1	1	2		
		18	2	1	1	2	1		
		16	2	1	2	1	1		
11	20720	19	2	2	2	0	1	8.02	-0.40
		17	1	2	2	1	1		
		14	2	2	0	2	1		

Table S18. Computed NEVPT2 transition energies and state-wise contribution to the axial and rhombic ZFS parameters of $[Co(L_1)]\cdot 2NO_3$ (**5**).

NEVPT2 excited states	Multiplicity	NEVPT2 energy (cm^{-1})	Contribution to D (cm^{-1})	Contribution to E (cm^{-1})
0	4	0	0.00	0.00
1	4	3575	-0.16	3.03
2	4	3965	0.37	-0.38
3	4	5186	13.65	14.12
4	4	6116	12.62	-12.61
5	4	13277	0.05	0.05
6	4	13580	0.04	-0.04
7	2	14654	-0.11	0.11
8	2	14867	0.09	-0.06
9	2	18501	0.18	-0.03
10	2	18551	-0.01	0.01
11	2	20720	8.02	-0.40
12	2	21186	2.09	-0.11
13	2	21272	0.30	0.06
14	4	21570	0.09	-0.09
15	2	21731	0.03	-1.20

16	2	21917	-1.50	1.50
17	4	22409	0.07	0.07
18	2	22629	0.00	0.00
19	4	22751	0.01	-0.01
20	2	23628	0.00	0.00
21	2	24591	0.00	0.00
22	2	27170	0.01	-0.01
23	2	27270	0.00	0.00
24	2	29624	-0.14	0.12
25	2	29852	-0.15	0.11
26	2	30120	-0.11	0.06
27	2	30130	-0.23	-0.21
28	2	31474	0.03	-0.02
29	2	31770	-0.02	0.02
30	2	32112	1.28	0.00
31	2	32545	-0.02	-0.02
32	2	32587	-0.01	0.01
33	2	33291	0.00	0.00
34	2	33663	-0.26	0.26
35	2	34001	-0.13	-0.17
36	2	35392	-0.37	-0.36
37	2	35673	-0.42	0.41
38	2	42825	-0.09	-0.05
39	2	42887	-0.08	0.01
40	2	43538	-0.08	-0.11
41	2	43715	-0.12	0.12
42	2	44203	-0.01	0.01
43	2	44324	0.00	0.00
44	2	44478	-0.01	0.01
45	2	64018	0.00	0.00
46	2	64309	0.00	0.00
47	2	64618	0.09	0.00
48	2	65647	0.06	0.00
49	2	65655	0.03	0.00

Table S19. Comparison of the calculated parameter for the magnetic anisotropy of $[Co(L_1)]\cdot 2ClO_4$ (**6**) at different levels of theory.

Calculated parameters	CASSCF	NEVPT2	Experimental values
D (cm^{-1})	37.17	31.34	26.00
E/D	0.15	0.14	0.00
g_z	2.05	2.23	-
g_y	2.36	2.27	-
g_x	2.47	2.36	-
g_{iso}	2.29	2.29	2.15

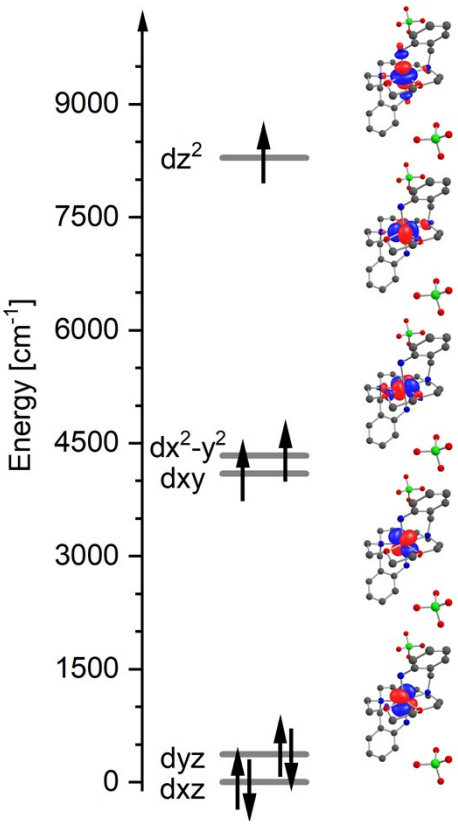

Figure S7. AILFT orbital energy diagram for $[Co(L_1)]\cdot 2ClO_4$ (**6**).

Table S20. Details of the major contributing excitations that lead to the D- and E-values (NEVPT2 level of theory) calculated for $[Co(L_1)]\cdot 2ClO_4$ (**6**).

NEVPT2 excited states	NEVPT2 energy (cm^{-1})	%	Major electronic configuration					Contribution to D (cm^{-1})	Contribution to E (cm^{-1})
			d_{xz} (0)	d_{yz} (372)	d_{xy} (4061)	$d_{x^2-y^2}$ (4335)	d_{z^2} (8286)		
0	0	84	2	2	1	1	1	0.00	0.00
		10	1	1	2	2	1		
1	3607	57	1	2	2	1	1	-0.10	3.03
		30	2	1	1	2	1		
2	3992	52	1	2	1	2	1	0.39	-0.41
		39	2	1	2	1	1		
3	5197	32	2	1	1	2	1	13.62	14.09
		23	1	2	1	2	1		
		18	1	2	1	1	2		
		17	2	1	2	1	1		
4	6130	27	1	2	2	1	1	12.59	-12.58
		20	2	1	1	2	1		
		20	2	1	1	1	2		
		18	2	1	2	1	1		
11	20663	24	2	2	2	0	1	9.10	-0.34
		22	2	2	0	2	1		

Table S21. Computed NEVPT2 transition energies and state-wise contribution to the axial and rhombic ZFS parameters of $[Co(L_1)]\cdot 2ClO_4$ (**6**).

NEVPT2 excited states	Multiplicity	NEVPT2 energy (cm^{-1})	Contribution to D (cm^{-1})	Contribution to E (cm^{-1})
0	4	0	0.00	0.00
1	4	3607	-0.10	3.03
2	4	3992	0.39	-0.41
3	4	5197	13.62	14.09
4	4	6130	12.59	-12.58
5	4	13286	0.05	0.05
6	4	13575	0.04	-0.04
7	2	14715	-0.11	0.11
8	2	14915	0.10	-0.06
9	2	18500	0.16	-0.02
10	2	18546	-0.01	0.01
11	2	20663	9.10	-0.34
12	2	21272	1.24	-0.15
13	2	21295	0.27	0.06
14	4	21564	0.09	-0.09
15	2	21758	-0.08	-1.22

16	2	21948	-1.50	1.50
17	4	22389	0.07	0.07
18	2	22635	0.00	0.00
19	4	22805	0.01	-0.01
20	2	23675	0.00	0.00
21	2	24638	0.00	0.00
22	2	27183	0.01	-0.01
23	2	27285	0.00	0.00
24	2	29577	-0.15	0.13
25	2	29825	-0.16	0.12
26	2	30100	-0.23	-0.22
27	2	30158	-0.09	0.05
28	2	31475	0.02	-0.02
29	2	31752	-0.02	0.01
30	2	32120	1.28	0.00
31	2	32551	-0.02	-0.02
32	2	32598	-0.01	0.01
33	2	33318	0.00	0.00
34	2	33680	-0.26	0.26
35	2	34014	-0.13	-0.17
36	2	35399	-0.37	-0.36
37	2	35680	-0.42	0.41
38	2	42843	-0.08	-0.04
39	2	42895	-0.07	0.00
40	2	43544	-0.09	-0.11
41	2	43725	-0.12	0.12
42	2	44231	0.00	0.00
43	2	44326	0.00	0.00
44	2	44477	-0.01	0.01
45	2	64035	0.00	0.00
46	2	64305	0.00	0.00
47	2	64629	0.08	0.00
48	2	65636	0.00	0.01
49	2	65691	0.10	0.00

Table S22. Comparison of the calculated parameter for the magnetic anisotropy of $[Co(L_2)]^{2+}$ (**7**) at different levels of theory.

Calculated parameters	CASSCF	NEVPT2	Experimental values
D (cm^{-1})	34.46	30.49	23.10
E/D	0.14	0.12	-
g_z	2.15	2.1	-
g_y	2.41	2.34	-
g_x	2.53	2.42	-
g_{iso}	2.36	2.29	2.21

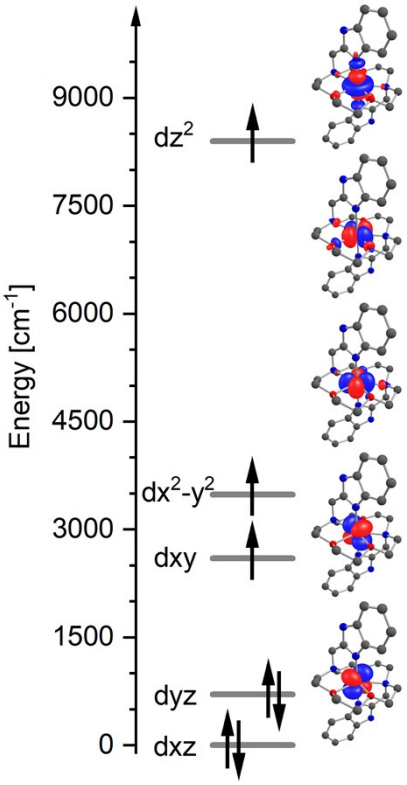

Figure S8. AILFT orbital energy diagram for $[Co(L_2)]^{2+}$ (**7**).

Table S23. Details of the major contributing excitations that lead to the D- and E-values (NEVPT2 level of theory) calculated for $[Co(L_2)]^{2+}$ (**7**).

NEVPT2 excited states	NEVPT2 energy (cm^{-1})	%	Major electronic configuration					Contribution to D (cm^{-1})	Contribution to E (cm^{-1})
			d_{xz} (0)	d_{yz} (707)	d_{xy} (2600)	$d_{x^2-y^2}$ (3486)	d_{z^2} (8399)		
$^4A_2'$	0	73	2	2	1	1	1	0.00	0.00
		11	1	1	2	2	1		
$^4E_2''$	2033	51	1	2	2	1	1	-1.30	5.06
		26	2	1	1	2	1		
		18	2	1	2	1	1		
	2582	44	1	2	1	2	1	-0.29	-0.08
		37	2	1	2	1	1		
$^4E_1''$	4644	46	2	1	1	2	1	13.73	12.96
		15	2	1	1	1	2		
		14	1	2	1	2	1		
$^4E_1''$	4753	25	1	2	1	2	1	15.41	-14.17
		19	1	2	2	1	1		
		15	2	1	2	1	1		
		14	1	2	1	1	2		
		34	2	2	1	1	1		
$^2A_1'$	20708	46	2	2	0	2	1	7.74	-0.11
		11	0	2	2	2	1		

Table S24. Computed NEVPT2 transition energies and state-wise contribution to the axial and rhombic ZFS parameters of $[Co(L_2)]^{2+}$ (**7**).

NEVPT2 excited states	Multiplicity	NEVPT2 energy (cm^{-1})	Contribution to D (cm^{-1})	Contribution to E (cm^{-1})
0	4	0	0.00	0.00
1	4	2033	-1.30	5.06
2	4	2582	-0.29	-0.08
3	4	4644	13.73	12.96
4	4	4753	15.41	-14.17
5	4	11276	0.17	0.13
6	4	12622	0.05	-0.04
7	2	13121	-0.24	0.21
8	2	14263	-0.07	-0.06
9	2	18128	2.60	-0.11
10	2	18766	0.00	0.00
11	4	19642	0.02	-0.02
12	2	19800	-0.32	-1.02
13	2	20314	-1.12	1.11

14	2	20354	-0.51	0.58
15	2	20572	-0.35	-0.55
16	2	20708	7.74	-0.11
17	4	21787	0.09	0.09
18	2	21880	0.00	0.00
19	4	22186	0.11	-0.11
20	2	22519	0.05	0.00
21	2	22657	0.00	0.00
22	2	26156	0.00	0.00
23	2	26272	-0.02	-0.04
24	2	28312	-0.14	0.13
25	2	29475	0.00	-0.01
26	2	29960	0.09	0.01
27	2	30167	-0.15	-0.06
28	2	30196	-0.02	0.02
29	2	30534	-0.15	-0.02
30	2	30787	1.41	-0.01
31	2	30981	-0.01	0.01
32	2	31474	0.00	-0.02
33	2	31582	0.10	0.01
34	2	32124	-0.29	0.28
35	2	32367	-0.03	-0.11
36	2	33246	-0.57	-0.57
37	2	34029	-0.43	0.43
38	2	41726	-0.24	-0.25
39	2	41958	-0.16	0.16
40	2	42294	-0.10	0.10
41	2	42987	0.04	0.00
42	2	43045	0.00	0.00
43	2	43584	0.00	-0.01
44	2	43853	0.00	0.00
45	2	62271	0.11	-0.01
46	2	62865	0.00	0.00
47	2	63381	0.07	0.00
48	2	64942	0.00	0.00
49	2	65293	-0.01	0.01

Table S25. Comparison of the calculated parameter for the magnetic anisotropy of $[Co(L_3)(H_2O)_2]^{2+}$ (**8**) at different levels of theory.

Calculated parameters	CASSCF	NEVPT2	Experimental values
D (cm^{-1})	41.53	35.15	24.60
E/D	0.02	0.02	0.00
g_z	2.00	2.00	-
g_y	2.38	2.3	-
g_x	2.40	2.31	-
g_{iso}	2.26	2.20	2.29

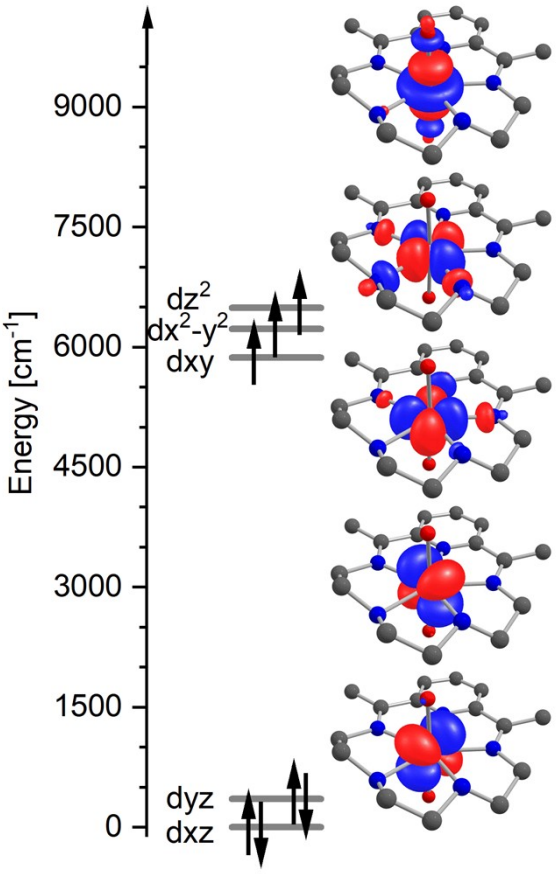

Figure S9. AILFT orbital energy diagram for $[Co(L_3)(H_2O)_2]^{2+}$ (**8**).

Table S26. Details of the major contributing excitations that lead to the D- and E-values (NEVPT2 level of theory) calculated for $[Co(L_3)(H_2O)_2]^{2+}$ (**8**).

NEVPT2 excited states	NEVPT2 energy (cm^{-1})	%	Major electronic configuration					Contribution to D (cm^{-1})	Contribution to E (cm^{-1})
			d_{xz} (0)	d_{yz} (353)	d_{xy} (5866)	$d_{x^2-y^2}$ (6224)	d_{z^2} (6492)		
$^4A_2$	0	90	2	2	1	1	1	0.00	0.00
$^4B_1$	5521.9	43	2	1	2	1	1	8.45	2.08
		30	1	2	2	1	1		
		14	2	1	1	1	2		
$^4B_2$	5780.2	34	2	1	2	1	1	12.01	2.12
		28	1	2	2	1	1		
		18	2	1	1	1	2		
		15	1	2	1	1	2		
$^4B_1$	6201.4	69	2	1	1	2	1	1.51	1.59
		22	1	2	2	1	1		
$^4B_1$	6458.6	73	1	2	1	2	1	6.02	-5.13
		17	1	2	1	1	2		
$^2A_1$	20905.5	50	2	2	0	2	1	13.17	-0.01
		24	2	2	2	0	1		

Table S27. Computed NEVPT2 transition energies and state-wise contribution to the axial and rhombic ZFS parameters of $[Co(L_3)(H_2O)_2]^{2+}$ (**8**).

NEVPT2 excited states	Multiplicity	NEVPT2 energy (cm^{-1})	Contribution to D (cm^{-1})	Contribution to E (cm^{-1})
0	4	0	0.00	0.00
1	4	5522	8.45	2.08
2	4	5780	12.01	2.12
3	4	6201	1.51	1.59
4	4	6459	6.02	-5.13
5	4	12966	0.01	0.00
6	4	13844	0.01	0.00
7	2	17868	0.49	0.00
8	2	18055	0.00	0.00
9	2	18356	-0.02	0.00
10	2	18921	0.04	0.00
11	4	20807	0.02	-0.01
12	2	20906	13.17	-0.01
13	4	21244	0.03	0.01
14	2	22646	0.00	0.00

15	2	22818	0.00	0.00
16	2	22825	0.05	0.00
17	2	23506	-1.50	-0.63
18	2	23634	-1.43	0.58
19	4	26887	0.00	0.00
20	2	27362	-0.07	0.04
21	2	27444	-0.11	-0.07
22	2	27651	-0.05	-0.02
23	2	27666	-0.03	-0.03
24	2	27709	-0.09	0.04
25	2	27921	-0.01	0.00
26	2	28799	-0.47	0.39
27	2	29099	-0.38	-0.34
28	2	31166	0.00	0.00
29	2	31672	0.00	0.00
30	2	32546	1.09	0.00
31	2	32585	0.04	0.00
32	2	32648	0.00	0.00
33	2	34218	-0.21	0.10
34	2	34475	-0.09	-0.05
35	2	34917	-0.01	-0.01
36	2	35289	-0.26	-0.01
37	2	35622	-0.37	0.00
38	2	42679	0.00	0.00
39	2	42687	0.01	0.00
40	2	44401	-0.01	0.00
41	2	44687	-0.02	0.00
42	2	46050	-0.11	-0.03
43	2	46077	-0.10	0.03
44	2	46562	0.00	0.00
45	2	63579	0.00	0.00
46	2	63748	0.00	0.00
47	2	66118	0.00	0.00
48	2	66342	0.00	0.00
49	2	68569	0.20	0.00

Table S28. Comparison of the calculated parameter for the magnetic anisotropy of [Co(L_4)Cl_2] (**9**) at different levels of theory.

Calculated parameters	CASSCF	NEVPT2	Experimental values
D (cm^{-1})	56.97	47.30	40.10
E/D	0.05	0.03	0.00
g_z	2.01	2.01	2.48
g_y	2.55	2.43	2.48
g_x	2.60	2.48	2.00
g_{iso}	2.38	2.31	2.32

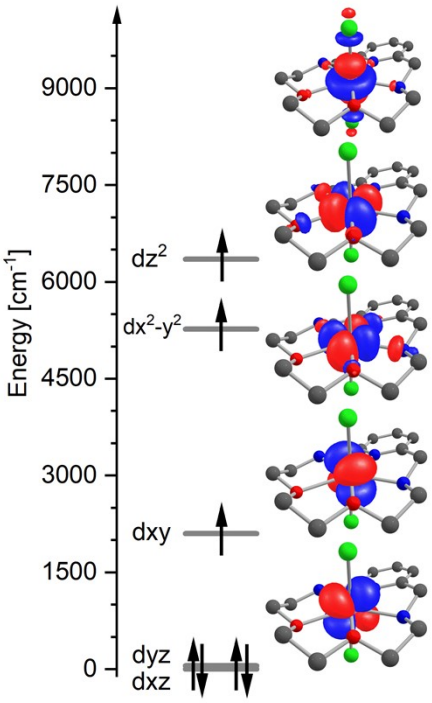

Figure S10. AILFT orbital energy diagram for [Co(L_4)Cl_2] (**9**).

Table S29. Details of the major contributing excitations that lead to the D- and E-values (NEVPT2 level of theory) calculated for $[Co(L_4)Cl_2]$ (**9**).

NEVPT2 excited states	NEVPT2 energy (cm^{-1})	%	Major electronic configuration					Contribution to D (cm^{-1})	Contribution to E (cm^{-1})
			d_{xz} (0)	d_{yz} (53)	d_{xy} (2102)	$d_{x^2-y^2}$ (5267)	d_{z^2} (6348)		
$^4A_2$	0	77	2	2	1	1	1	0.00	0.00
$^4B_1$	2177	54	1	2	1	2	1	12.01	-10.88
		16	2	1	1	2	1		
		14	2	1	2	1	1		
$^4B_2$	2269	49	2	1	1	2	1	12.28	12.30
		17	1	2	1	2	1		
		15	1	2	2	1	1		
$^4B_1$	5280	43	1	2	2	1	1	8.60	9.66
		17	2	1	2	1	1		
		16	1	2	1	1	2		
$^4B_2$	6005	40	2	1	2	1	1	9.12	-8.96
		19	1	2	2	1	1		
		17	2	1	1	1	2		
		10	2	1	1	2	1		
$^2A_1$	15539	45	2	2	0	2	1	5.24	-0.12
		30	2	2	1	1	1		
$^2A_1$	22404	38	2	2	2	0	1	6.27	-0.01
		16	1	1	1	2	2		
		12	2	2	1	1	1		

Table S30. Computed NEVPT2 transition energies and state-wise contribution to the axial and rhombic ZFS parameters of $[Co(L_4)Cl_2]$ (**9**).

NEVPT2 excited states	Multiplicity	NEVPT2 energy (cm^{-1})	Contribution to D (cm^{-1})	Contribution to E (cm^{-1})
0	4	0	0.00	0.00
1	4	2177	12.01	-10.88
2	4	2269	12.28	12.30
3	4	5280	8.60	9.66
4	4	6005	9.12	-8.96
5	4	9071	0.09	-0.08
6	4	13038	0.00	0.01
7	2	14086	0.67	-0.04
8	2	15539	5.24	-0.12
9	2	17499	-0.02	0.02
10	2	18365	-0.01	0.00

11	2	19927	-0.03	0.03
12	4	20201	0.04	-0.04
13	2	20399	-0.01	-0.08
14	2	20438	-1.43	-1.46
15	2	20481	-1.49	1.48
16	4	20690	0.04	0.04
17	4	21721	0.00	0.00
18	2	22124	0.00	0.00
19	2	22404	6.27	-0.01
20	2	23419	0.00	0.00
21	2	23525	-0.05	-0.05
22	2	26671	-0.31	0.29
23	2	26771	-0.17	-0.17
24	2	26975	-0.08	-0.04
25	2	27220	-0.06	-0.01
26	2	28130	0.00	0.00
27	2	29544	-0.02	0.01
28	2	29692	0.83	-0.03
29	2	30139	-0.12	0.15
30	2	30455	-0.07	-0.14
31	2	30485	0.00	-0.01
32	2	31425	1.32	0.00
33	2	31809	-0.11	-0.11
34	2	32144	-0.24	0.23
35	2	32394	-0.01	0.01
36	2	32988	-0.39	0.20
37	2	33060	-0.44	-0.24
38	2	41503	0.00	-0.03
39	2	41846	0.00	0.00
40	2	42040	-0.08	0.08
41	2	42297	-0.16	-0.06
42	2	42399	-0.12	0.00
43	2	42802	0.00	0.00
44	2	43359	0.00	0.00
45	2	62831	-0.01	-0.01
46	2	62831	0.00	0.00
47	2	62860	0.00	0.00
48	2	63181	0.00	0.00
49	2	64060	0.20	0.00

Table S31. Comparison of the calculated parameter for the magnetic anisotropy of $[Co(L_5H_2)I(H_2O)]$ (**10**) at different levels of theory.

Calculated parameters	CASSCF	NEVPT2	Experimental values
D (cm^{-1})	44.11	36.97	30.00
E/D	0.03	0.03	0.01
g_z	1.99	2.00	-
g_y	2.43	2.32	-
g_x	2.48	2.34	-
g_{iso}	2.30	2.24	2.24

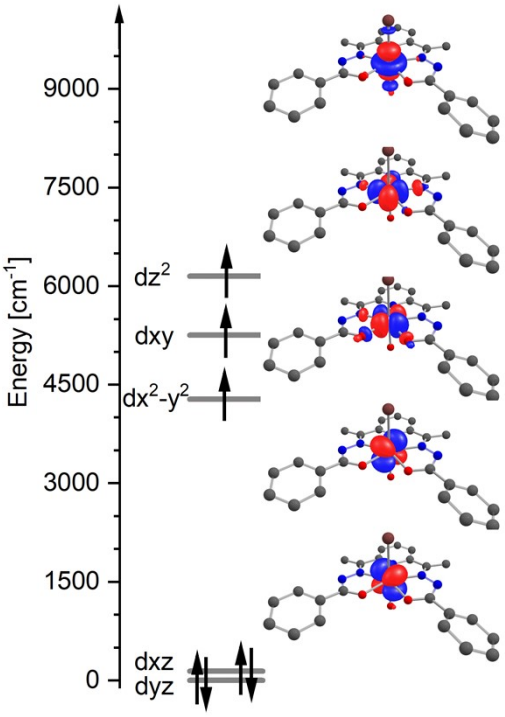

Figure S11. AILFT orbital energy diagram for $[Co(L_5H_2)I(H_2O)]^+$ (**10**).

Table S32. Details of the major contributing excitations that lead to the D- and E-values (NEVPT2 level of theory) calculated for $[Co(L_5H_2)I(H_2O)]^+$ (**10**).

NEVPT2 excited states	NEVPT2 energy (cm^{-1})	%	Major electronic configuration					Contribution to D (cm^{-1})	Contribution to E (cm^{-1})
			d_{xz} (0)	d_{yz} (144)	d_{xy} (4277)	$d_{x^2-y^2}$ (5254)	d_{z^2} (6152)		
$^4A_2$	0	89	2	2	1	1	1	0.00	0.00
$^4B_1$	4222	77	2	1	1	2	1	3.77	-2.79
		13	2	1	1	1	2		
$^4B_2$	4388	71	1	2	1	2	1	3.09	2.70
		18	2	1	2	1	1		
$^4B_1$	5423	40	2	1	2	1	1	12.57	11.55
		27	1	2	2	1	1		
		15	1	2	1	1	2		
		14	2	1	1	1	2		
$^4B_2$	5858	43	1	2	2	1	1	11.04	-10.45
		18	2	1	2	1	1		
		17	1	2	1	1	2		
		10	1	2	1	2	1		
$^2A_1$	21147	53	2	2	2	0	1	7.44	0.00
		15	2	2	0	2	1		

Table S33. Computed NEVPT2 transition energies and state-wise contribution to the axial and rhombic ZFS parameters of $[Co(L_5H_2)I(H_2O)]$ (**10**).

NEVPT2 excited states	Multiplicity	NEVPT2 energy (cm^{-1})	Contribution to D (cm^{-1})	Contribution to E (cm^{-1})
0	4	0	0	0
1	4	4222.5	3.772	-2.785
2	4	4387.9	3.092	2.698
3	4	5422.9	12.568	11.551
4	4	5858.3	11.041	-10.446
5	4	12206.4	0.006	-0.005
6	4	13428.4	0.001	0.001
7	2	15814.7	0.02	-0.008
8	2	16867.2	0.017	0.005
9	2	17723.2	1.667	0.002
10	2	18234.3	-0.004	-0.004
11	4	20695.2	0.025	-0.022
12	2	21146.9	7.439	0.003
13	4	21101.9	0.022	0.017
14	2	21730.8	0.079	-0.019
15	2	21861.6	0.025	0.002

16	2	22119.1	-1.516	-1.376
17	2	22317.5	-1.373	1.312
18	2	22335.4	-0.001	-0.001
19	4	24104.9	0.00	0.00
20	2	24984.1	-0.009	0.012
21	2	25382.7	-0.009	-0.006
22	2	27138.5	-0.015	0.016
23	2	27240.4	-0.036	-0.036
24	2	28580.6	-0.079	0.077
25	2	28733.2	-0.05	-0.046
26	2	29077.1	-0.286	0.27
27	2	29120.7	-0.068	0.053
28	2	30066.8	-0.307	-0.302
29	2	31345.5	0	-0.006
30	2	31750.2	0.079	0
31	2	31839.1	0.057	-0.003
32	2	31840.6	1.321	0.001
33	2	33344.3	-0.002	0
34	2	33514.3	-0.029	-0.017
35	2	33575.1	-0.049	0.038
36	2	34454.5	-0.447	0.135
37	2	34723.3	-0.433	-0.108
38	2	42305.4	0.001	0.001
39	2	42348.3	0.002	0
40	2	43465	-0.008	0.001
41	2	43660.5	-0.112	-0.085
42	2	43857.5	-0.128	0.08
43	2	43981.4	-0.019	-0.002
44	2	44438	0	0
45	2	63256.9	0.001	0
46	2	63362.4	0	0
47	2	64217.7	-0.002	-0.002
48	2	64528.1	0.001	0.002
49	2	65902.7	0.206	0

Table S34. Comparison of the calculated parameter for the magnetic anisotropy of $[Co(L_5H_2)(H_2O)(NO_3)]$ (**11**) at different levels of theory

Calculated parameters	CASSCF	NEVPT2	Experimental values
D (cm^{-1})	41.58	35.50	31.00
E/D	0.08	0.07	0.00
g_z	2.02	2.01	-
g_y	2.39	2.30	-
g_x	2.46	2.36	-
g_{iso}	2.29	2.23	2.22

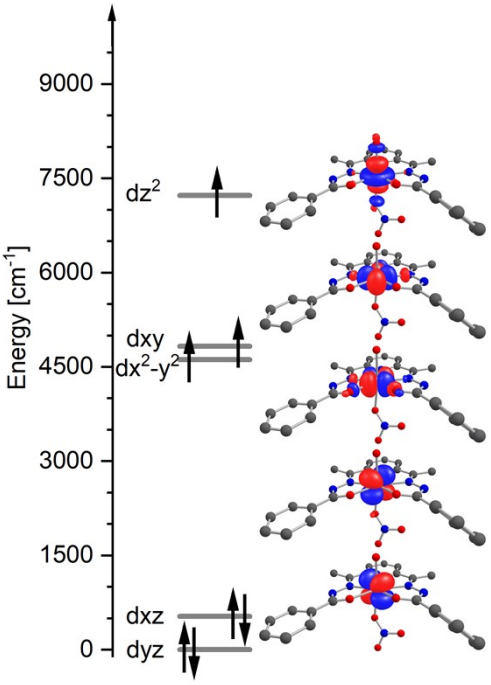

Figure S12. AILFT orbital energy diagram for $[Co(L_5H_2)(H_2O)(NO_3)]$ (**11**).

Table S35. Details of the major contributing excitations that lead to the D- and E-values (NEVPT2 level of theory) calculated for $[Co(L_5H_2)(H_2O)(NO_3)]$ (**11**).

NEVPT2 excited states	NEVPT2 energy (cm^{-1})	%	Major electronic configuration					Contribution to D (cm^{-1})	Contribution to E (cm^{-1})
			d_{xz} (0)	d_{yz} (531)	d_{xy} (4614)	$d_{x^2-y^2}$ (4828)	d_{z^2} (7225)		
$^4A_2'$	0	87	2	2	1	1	1	0.00	0.00
$^4E_2''$	4039	39	2	1	1	2	1	4.34	5.07
		31	2	1	2	1	1		
		20	1	2	2	1	1		
	4342	41	1	2	1	2	1	0.03	-0.71
		37	2	1	2	1	1		
		17	2	1	1	2	1		
$^4E_1''$	5361	37	1	2	1	2	1	11.87	11.95
		26	2	1	1	1	2		
		16	1	2	2	1	1		
		14	2	1	2	1	1		
	5812	43	1	2	2	1	1	13.52	-13.53
		30	1	2	1	1	2		
		20	2	1	1	2	1		
$^2A_1'$	20577	35	2	2	2	0	1	12.58	0.00
		33	2	2	0	2	1		
		11	2	0	2	2	1		

Table S36. Computed NEVPT2 transition energies and state-wise contribution to the axial and rhombic ZFS parameters of $[Co(L_5H_2)(H_2O)(NO_3)]$ (**11**).

NEVPT2 excited states	Multiplicity	NEVPT2 energy (cm^{-1})	Contribution to D (cm^{-1})	Contribution to E (cm^{-1})
0	4	0	0.00	0.00
1	4	4039	4.34	5.07
2	4	4342	0.03	-0.71
3	4	5361	11.87	11.95
4	4	5812	13.52	-13.53
5	4	12573	0.04	-0.01
6	4	12963	0.01	0.00
7	2	16376	-0.02	0.00
8	2	16655	0.01	0.00
9	2	18393	0.16	0.00
10	2	18437	-0.02	-0.01
11	2	20577	12.58	0.00
12	4	21098	0.06	-0.02
13	4	21521	0.06	0.01

14	2	21729	-0.12	-0.11
15	2	21902	0.21	0.02
16	2	22195	-1.45	-1.17
17	2	22332	-1.47	1.15
18	2	22798	0.00	0.00
19	4	23649	0.00	0.00
20	2	24844	0.01	0.00
21	2	25625	0.00	0.00
22	2	27105	-0.01	-0.01
23	2	27226	0.00	0.00
24	2	28588	-0.39	0.38
25	2	29221	-0.33	-0.30
26	2	29359	-0.04	0.01
27	2	29617	0.00	0.00
28	2	30770	-0.02	-0.04
29	2	31196	-0.04	0.00
30	2	31585	1.37	0.00
31	2	31860	0.00	0.00
32	2	32083	0.01	0.00
33	2	33275	-0.01	-0.01
34	2	33496	-0.18	0.11
35	2	33617	-0.13	-0.08
36	2	34615	-0.38	-0.23
37	2	35096	-0.44	0.29
38	2	42740	0.00	0.00
39	2	42766	0.02	-0.01
40	2	43681	-0.16	-0.10
41	2	43862	-0.15	0.07
42	2	44049	-0.01	0.00
43	2	44232	-0.02	0.02
44	2	44563	0.00	0.00
45	2	63851	0.01	0.00
46	2	64041	0.00	0.00
47	2	64723	0.00	0.00
48	2	65130	0.01	0.00
49	2	66017	0.19	0.00

Table S37. Comparison of the calculated parameter for the magnetic anisotropy of $[Co(L_5H)(H_2O)(EtOH)]^+$ (**12**) at different levels of theory.

Calculated parameters	CASSCF	NEVPT2	Experimental values
D (cm^{-1})	44.07	37.51	27.65
E/D	0.01	0.00	0.00
g_z	1.99	2.00	-
g_y	2.42	2.33	-
g_x	2.43	2.34	-
g_{iso}	2.28	2.22	2.25

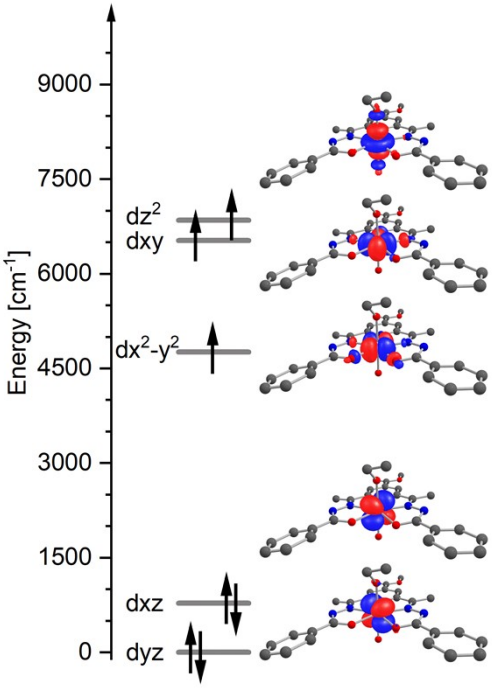

Figure S13. AILFT orbital energy diagram for $[Co(L_5H)(H_2O)(EtOH)]^+$ (**12**).

Table S38. Details of the major contributing excitations that lead to the D- and E-values (NEVPT2 level of theory) calculated for $[Co(L_5H)(H_2O)(EtOH)]^+$ (**12**).

NEVPT2 excited states	NEVPT2 energy (cm^{-1})	%	Major electronic configuration					Contribution to D (cm^{-1})	Contribution to E (cm^{-1})
			d_{xz} (0)	d_{yz} (781)	d_{xy} (4761)	$d_{x^2-y^2}$ (6526)	d_{z^2} (6845)		
$^4A_2$	0	90	2	2	1	1	1	0.00	0.00
$^4B_1$	4105	55	1	2	2	1	1	7.58	-4.53
		18	1	2	1	2	1		
		12	2	1	1	2	1		
$^4B_2$	4785	57	2	1	2	1	1	5.76	3.88
		15	2	1	1	2	1		
		14	1	2	1	2	1		
$^4B_1$	5746	44	1	2	1	2	1	9.88	6.32
		22	1	2	2	1	1		
		17	1	2	1	1	2		
$^4B_2$	6751	45	2	1	1	2	1	8.05	-5.24
		20	1	2	1	2	1		
		16	2	1	1	1	2		
$^2A_1$	16932	57	2	2	1	1	1	2.86	0.00
		25	2	2	2	0	1		
$^2A_1$	21675	39	2	2	0	2	1	10.16	0.02
		18	2	2	2	0	1		
		12	2	2	1	1	1		

Table S39. Computed NEVPT2 transition energies and state-wise contribution to the axial and rhombic ZFS parameters of $[Co(L_5H)(H_2O)(EtOH)]^+$ (**12**).

NEVPT2 excited states	Multiplicity	NEVPT2 energy (cm^{-1})	Contribution to D (cm^{-1})	Contribution to E (cm^{-1})
0	4	0	0.00	0.00
1	4	4105	7.58	-4.53
2	4	4785	5.76	3.88
3	4	5746	9.88	6.32
4	4	6751	8.05	-5.24
5	4	11917	0.01	-0.01
6	4	14119	0.00	0.00
7	2	16759	0.34	-0.01
8	2	16932	2.86	0.00
9	2	18232	0.00	0.00
10	2	18468	0.05	0.01
11	4	20589	0.04	-0.01

12	4	21549	0.05	0.01
13	2	21675	10.16	0.02
14	2	22031	-0.01	0.01
15	2	22253	0.08	-0.06
16	2	22394	-1.35	0.33
17	2	22661	0.00	0.00
18	2	22835	-1.46	-0.36
19	4	25272	0.00	0.00
20	2	25491	-0.12	0.01
21	2	25927	-0.07	-0.03
22	2	27748	-0.03	-0.03
23	2	28069	-0.07	0.02
24	2	28170	-0.12	0.10
25	2	28391	-0.02	-0.02
26	2	29567	-0.30	0.07
27	2	29688	-0.32	0.00
28	2	30437	-0.01	0.00
29	2	31258	0.25	-0.03
30	2	31970	0.04	0.00
31	2	32124	0.04	-0.01
32	2	32594	1.01	0.00
33	2	33963	-0.07	-0.05
34	2	34012	-0.01	0.00
35	2	34492	-0.20	0.17
36	2	34566	-0.26	-0.05
37	2	35416	-0.47	-0.06
38	2	42705	0.00	0.00
39	2	42717	0.00	0.00
40	2	43718	0.00	0.00
41	2	44618	-0.06	-0.03
42	2	44842	-0.07	-0.02
43	2	44993	-0.14	0.04
44	2	45561	0.00	0.00
45	2	63712	0.01	0.00
46	2	63863	0.00	0.00
47	2	65291	0.00	0.00
48	2	65775	0.00	0.00
49	2	67392	0.21	0.00

Table S40. Comparison of the calculated parameters for the magnetic anisotropy of [Co(L_5)(H_2O)] (**13**) at different levels of theory.

Calculated parameters	CASSCF	NEVPT2	Experimental values
D (cm^{-1})	40.36	34.37	13.10
E/D	0.07	0.06	0.00
g_z	2.01	2.01	-
g_y	2.35	2.28	-
g_x	2.42	2.32	-
g_{iso}	2.26	2.20	2.06

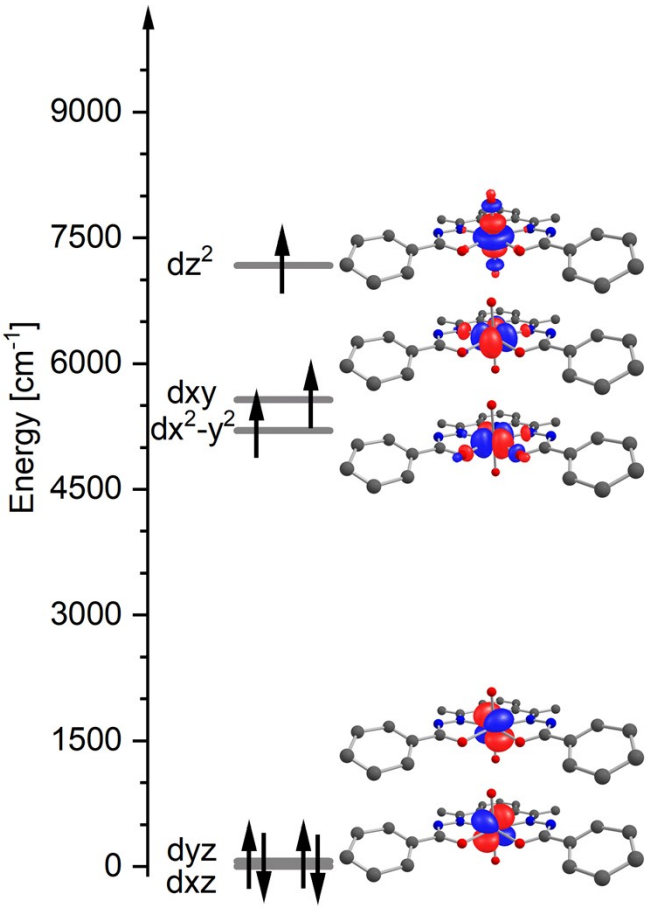

Figure S14. AILFT orbital energy diagram for [Co(L_5)(H_2O)] (**13**).

Table S41. Details of the major contributing excitations that lead to the D- and E-values (NEVPT2 level of theory) calculated for [Co(L_5)(H_2O)] (**13**).

NEVPT2 excited states	NEVPT2 energy (cm^{-1})	%	Major electronic configuration					Contribution to D (cm^{-1})	Contribution to E (cm^{-1})
			d_{xz} (0)	d_{yz} (66)	d_{xy} (5202)	$d_{x^2-y^2}$ (5570)	d_{z^2} (7169)		
$^4A_2'$	0	90	2	1	1	2	1	0.00	0.00
$^4E_2''$	5157	43	1	2	2	1	1	1.68	-2.22
		30	2	1	2	1	1		
		20	2	1	1	2	1		
	5477	41	2	1	2	1	1	0.47	0.47
		27	1	2	1	2	1		
		21	1	2	2	1	1		
$^4E_1''$	5628	22	2	2	1	1	1	14.63	14.53
		22	2	1	2	1	1		
		20	1	2	1	2	1		
		18	1	2	1	2	1		
		13	1	1	2	2	1		
	6568	32	1	2	1	2	1	10.60	-10.75
		30	2	2	1	1	1		
		18	1	1	2	2	1		
		12	2	1	2	1	1		
$^2A_1'$	20841	49	2	2	1	2	0	12.98	0.00
		24	2	0	1	2	2		

Table S42. Computed NEVPT2 transition energies and state-wise contribution to the axial and rhombic ZFS parameters of [Co(L_5)(H_2O)] (**13**).

NEVPT2 excited states	Multiplicity	NEVPT2 energy (cm^{-1})	Contribution to D (cm^{-1})	Contribution to E (cm^{-1})
0	4	0	0.00	0.00
1	4	5157	1.68	-2.22
2	4	5477	0.47	0.47
3	4	5628	14.63	14.53
4	4	6568	10.60	-10.75
5	4	13550	0.01	0.01
6	4	14148	0.01	-0.01
7	2	16958	0.33	0.04
8	2	17534	-0.01	-0.01
9	2	18224	0.28	0.00
10	2	18299	-0.03	-0.03
11	2	20841	12.98	0.00
12	4	21206	0.05	-0.05
13	4	21905	0.05	0.05

14	2	22580	0.04	0.00
15	2	22596	0.07	0.00
16	2	22902	0.00	0.00
17	2	23012	-1.58	-1.58
18	2	23273	-1.45	1.46
19	4	25630	0.00	0.00
20	2	26195	0.00	0.00
21	2	26762	-0.05	-0.05
22	2	27555	-0.01	-0.01
23	2	27850	-0.01	0.02
24	2	28827	-0.49	0.49
25	2	29351	-0.03	-0.03
26	2	29429	-0.02	0.02
27	2	29476	-0.37	-0.36
28	2	31654	-0.01	-0.01
29	2	32012	0.01	0.01
30	2	32794	1.12	0.00
31	2	33015	0.04	0.00
32	2	33028	0.00	0.00
33	2	34481	-0.16	0.16
34	2	34584	-0.10	-0.10
35	2	34922	0.00	0.00
36	2	35750	-0.41	0.39
37	2	35941	-0.39	-0.36
38	2	43040	0.00	0.00
39	2	43082	0.01	0.00
40	2	44466	-0.03	-0.03
41	2	44704	-0.03	0.03
42	2	45236	-0.12	-0.12
43	2	45425	-0.10	0.10
44	2	45983	0.00	0.00
45	2	64275	0.00	0.00
46	2	64391	0.00	0.00
47	2	65644	0.00	0.00
48	2	66227	0.00	0.00
49	2	67656	0.20	0.00

Table S43. Comparison of the calculated parameters for the magnetic anisotropy of $[Co(L_5)(im)_2]$ (**14**) at different levels of theory.

Calculated parameters	CASSCF	NEVPT2	Experimental values
D (cm^{-1})	41.32	35.00	24.80
E/D	0.08	0.06	0.00
g_z	1.99	2.00	-
g_y	2.35	2.27	-
g_x	2.42	2.32	-
g_{iso}	2.26	2.20	2.21

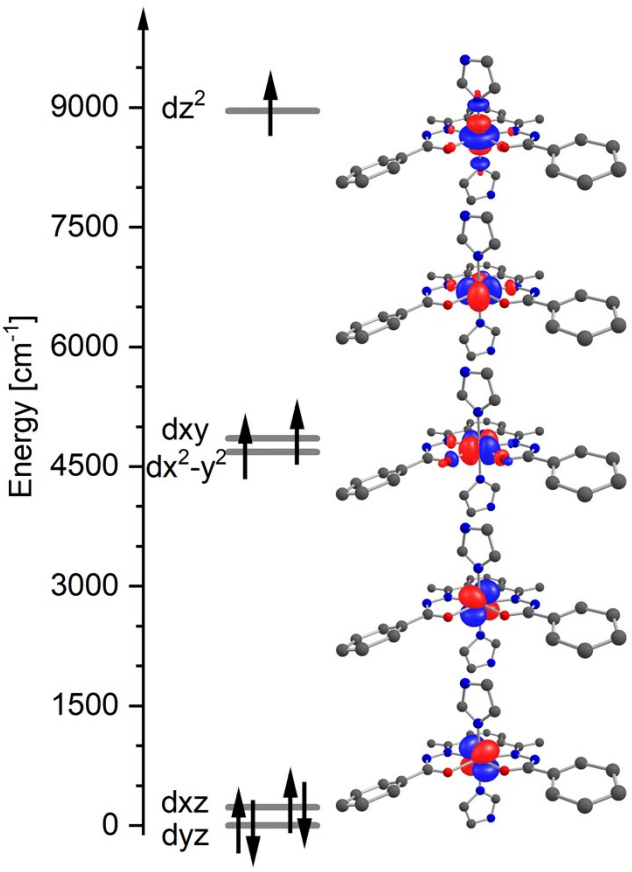

Figure S15. AILFT orbital energy diagram for $[Co(L_5)(im)_2]$ (**14**).

Table S44. Details of the major contributing excitations that lead to the D- and E-values (NEVPT2 level of theory) calculated for [Co(L_5)(im)$_2$] (**14**).

NEVPT2 excited states	NEVPT2 energy (cm^{-1})	%	Major electronic configuration					Contribution to D (cm^{-1})	Contribution to E (cm^{-1})
			d_{xz} (0)	d_{yz} (232)	d_{xy} (4683)	$d_{x^2-y^2}$ (4854)	d_{z^2} (8958)		
$^4A_2'$	0	89	2	2	1	1	1	0.00	0.00
$^4E_2''$	4454	44	2	1	2	1	1	0.74	-0.74
		25	1	2	1	2	1		
		21	1	2	2	1	1		
	4476	43	2	1	1	2	1	0.31	0.53
		28	1	2	2	1	1		
		19	1	2	1	2	1		
$^4E_1''$	5781	25	2	1	2	1	1	14.43	14.43
		22	1	2	2	1	1		
		17	2	1	1	1	2		
		14	1	2	1	2	1		
		13	1	2	1	1	2		
	6618	27	2	1	1	2	1	12.03	-12.03
		25	1	2	1	2	1		
		16	1	2	1	1	2		
		13	1	2	2	1	1		
		12	2	1	1	1	2		
$^2A_1'$	20494	42	2	2	0	2	1	13.65	0.00
		29	2	2	2	0	1		
		10	2	0	2	2	1		
		10	0	2	2	2	1		

Table S45. Computed NEVPT2 transition energies and state-wise contribution to the axial and rhombic ZFS parameters of [Co(L_5)(im)$_2$] (**14**).

NEVPT2 excited states	Multiplicity	NEVPT2 energy (cm^{-1})	Contribution to D (cm^{-1})	Contribution to E (cm^{-1})
0	4	0	0.00	0.00
1	4	4454	0.74	-0.74
2	4	4476	0.31	0.53
3	4	5781	14.43	14.43
4	4	6618	12.03	-12.03
5	2	14576	0.10	-0.01
6	2	14781	-0.01	0.01
7	4	14925	0.00	0.00
8	4	15142	0.00	0.00
9	2	18332	0.09	0.00
10	2	18343	0.00	0.00

11	2	20494	13.65	0.00
12	2	22117	-0.22	0.22
13	2	22179	-0.44	-0.45
14	4	22284	0.12	-0.12
15	2	22329	-1.16	-1.17
16	2	22497	-1.28	1.28
17	2	22610	0.00	0.00
18	4	22825	0.10	0.10
19	4	23960	0.00	0.00
20	2	24361	0.00	0.00
21	2	25081	0.00	0.00
22	2	27743	0.00	0.00
23	2	27796	0.00	0.00
24	2	29779	-0.28	0.28
25	2	30505	-0.19	-0.19
26	2	30913	-0.10	-0.10
27	2	31180	-0.07	0.07
28	2	32576	0.00	0.00
29	2	32612	0.03	-0.01
30	2	33357	1.16	0.00
31	2	34148	0.01	0.00
32	2	34166	0.00	0.00
33	2	34636	0.00	0.00
34	2	35063	-0.02	0.02
35	2	35133	0.01	-0.02
36	2	36679	-0.52	-0.52
37	2	36705	-0.62	0.62
38	2	43500	-0.05	-0.05
39	2	43620	-0.03	0.03
40	2	44190	-0.15	-0.15
41	2	44394	-0.16	0.16
42	2	44867	0.00	0.00
43	2	44901	0.00	0.00
44	2	45206	0.00	0.00
45	2	65103	0.03	0.00
46	2	65186	0.00	0.00
47	2	65202	0.01	0.00
48	2	65795	0.00	0.00
49	2	66212	0.18	0.00

Table S46. Comparison of the calculated parameters for the magnetic anisotropy of $[Co(L_5H_2)(NCS)_2]$ (**15**) at different levels of theory.

Calculated parameters	CASSCF	NEVPT2	Experimental values
D (cm^{-1})	44.17	38.07	15.90
E/D	0.06	0.05	0.00
g_z	2.01	2.01	-
g_y	2.43	2.34	-
g_x	2.48	2.38	-
g_{iso}	2.31	2.24	2.14

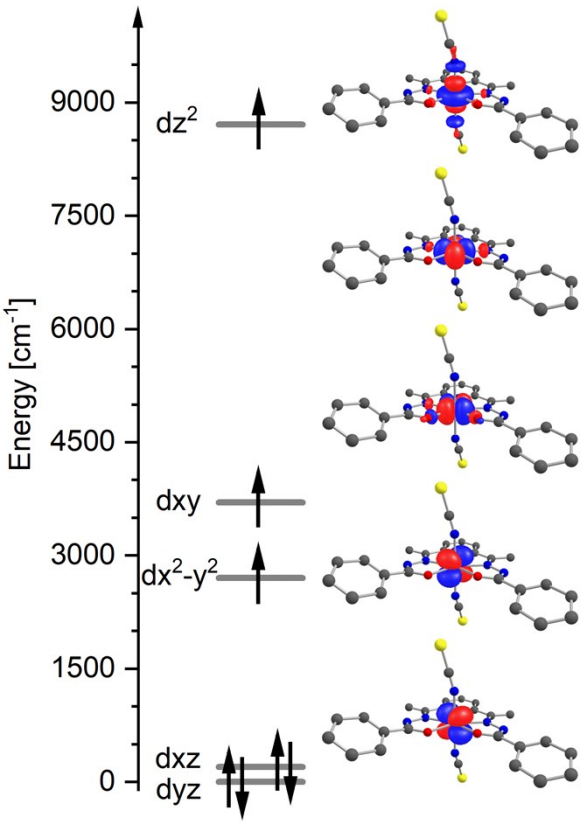

Figure S16. AILFT orbital energy diagram for $[Co(L_5H_2)(NCS)_2]$ (**15**).

Table S47. Details of the major contributing excitations that lead to the D- and E-values (NEVPT2 level of theory) calculated for $[Co(L_5H_2)(NCS)_2]$ (**15**).

NEVPT2 excited states	NEVPT2 energy (cm^{-1})	%	Major electronic configuration					Contribution to D (cm^{-1})	Contribution to E (cm^{-1})
			d_{xz} (0)	d_{yz} (200)	d_{xy} (2704)	$d_{x^2-y^2}$ (3703)	d_{z^2} (8707)		
$^4A_2'$	0	86	2	2	1	1	1	0.00	0.00
		12	1	1	2	2	1		
$^4E_2''$	2676	47	2	1	2	1	1	1.34	-0.43
		30	1	2	1	2	1		
		19	1	2	2	1	1		
	2849	47	1	2	2	1	1	0.07	0.44
		32	2	1	1	2	1		
		14	2	1	2	1	1		
$^4E_1''$	4789	33	2	1	1	2	1	17.03	15.21
		17	2	1	2	1	1		
		16	1	2	1	1	2		
		12	1	2	1	2	1		
		11	2	1	1	1	2		
		10	1	2	2	1	1		
	5314	38	1	2	1	2	1	14.49	-13.32
		18	2	1	1	2	1		
		15	2	1	1	1	2		
		10	1	2	1	1	2		
$^2A_1'$	20574	54	2	2	0	2	1	9.64	0.08

Table S48. Computed NEVPT2 transition energies and state-wise contribution to the axial and rhombic ZFS parameters of $[Co(L_5H_2)(NCS)_2]$ (**15**).

NEVPT2 excited states	Multiplicity	NEVPT2 energy (cm^{-1})	Contribution to D (cm^{-1})	Contribution to E (cm^{-1})
0	4	0	0.00	0.00
1	4	2676	1.34	-0.43
2	4	2849	0.07	0.44
3	4	4789	17.03	15.21
4	4	5314	14.49	-13.32
5	4	12574	0.03	-0.02
6	2	12927	-0.03	-0.01
7	4	13752	0.01	0.01
8	2	14007	-0.01	0.01
9	2	17990	2.63	0.01
10	2	18579	0.00	0.00
11	2	20376	-0.99	-0.15
12	2	20574	9.64	0.08

13	2	20595	-1.29	-0.12
14	4	20645	0.00	0.00
15	2	20952	-0.21	-0.17
16	2	20971	-0.15	0.30
17	4	22044	0.14	-0.13
18	4	22402	0.13	0.11
19	2	22429	0.00	0.00
20	2	22444	0.00	0.00
21	2	22847	0.00	0.00
22	2	26576	-0.01	0.00
23	2	26600	-0.01	0.01
24	2	28997	-0.18	0.06
25	2	29275	-0.16	-0.07
26	2	30320	-0.03	0.03
27	2	31127	0.03	0.00
28	2	31611	-0.04	-0.04
29	2	31637	-0.01	0.03
30	2	31953	0.90	0.00
31	2	32061	0.51	0.00
32	2	32107	-0.02	-0.02
33	2	32196	0.11	0.02
34	2	32759	-0.07	0.06
35	2	32913	-0.03	-0.04
36	2	34589	-0.60	-0.06
37	2	34738	-0.61	0.12
38	2	42108	-0.26	-0.15
39	2	42277	-0.26	0.13
40	2	43057	0.00	0.00
41	2	43253	0.00	0.00
42	2	43315	-0.01	0.01
43	2	43840	0.00	0.00
44	2	44118	0.00	0.00
45	2	63242	0.21	0.00
46	2	63520	0.00	0.00
47	2	63826	0.00	0.00
48	2	64735	0.00	0.00
49	2	64839	0.00	0.00

Table S49. Comparison of the calculated parameters for the magnetic anisotropy of $[Co(NO_3)(EtOH)]^+$ (**16**) at different levels of theory.

Calculated parameters	CASSCF	NEVPT2	Experimental values
D (cm^{-1})	44.79	38.21	33.00
E/D	0.02	0.01	0.00
g_z	1.99	2.00	-
g_y	2.42	2.33	-
g_x	2.44	2.35	-
g_{iso}	2.29	2.23	2.25

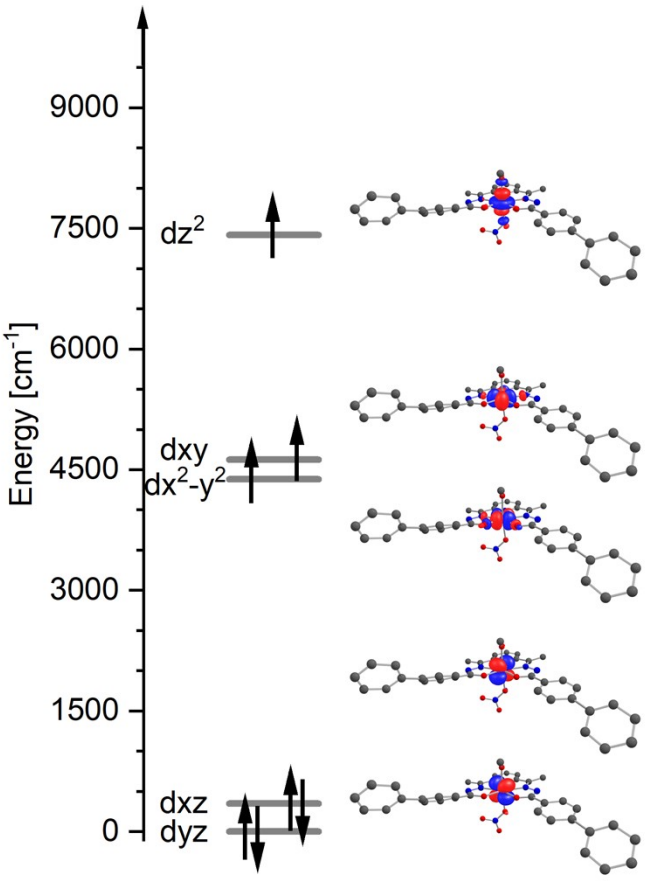

Figure S17. AILFT orbital energy diagram for $[Co(NO_3)(EtOH)]^+$ (**16**).

Table S50. Details of the major contributing excitations that lead to the D- and E-values (NEVPT2 level of theory) calculated for $[Co(NO_3)(EtOH)]^+$ (**16**).

NEVPT2 excited states	NEVPT2 energy (cm^{-1})	%	Major electronic configuration					Contribution to D (cm^{-1})	Contribution to E (cm^{-1})
			d_{xz} (0)	d_{yz} (348)	d_{xy} (4383)	$d_{x^2-y^2}$ (4626)	d_{z^2} (7418)		
$^4A_2'$	0	88	2	2	1	1	1	0.00	0.00
$^4E_2''$	4026	50	2	1	1	2	1	1.36	-0.70
		16	1	2	1	2	1		
		16	1	2	2	1	1		
		15	2	1	2	1	1		
	4137	36	2	1	2	1	1	-0.26	-0.02
		29	1	2	1	2	1		
		18	1	2	2	1	1		
		16	2	1	1	2	1		
$^4E_1''$	5263	32	2	1	2	1	1	16.12	14.50
		31	2	1	1	1	2		
		29	1	2	1	2	1		
	5520	44	1	2	2	1	1	14.48	-13.25
		29	1	2	1	1	2		
		17	2	1	1	2	1		
$^2A_1'$	20441	41	2	2	2	0	1	13.24	0.00
		27	2	2	0	2	1		
		11	2	0	2	2	1		

Table S51. Computed NEVPT2 transition energies and state-wise contribution to the axial and rhombic ZFS parameters of $[Co(NO_3)(EtOH)]^+$ (**16**).

NEVPT2 excited states	Multiplicity	NEVPT2 energy (cm^{-1})	Contribution to D (cm^{-1})	Contribution to E (cm^{-1})
0	4	0	0.00	0.00
1	4	4026	1.36	-0.70
2	4	4137	-0.26	-0.02
3	4	5263	16.12	14.50
4	4	5520	14.48	-13.25
5	4	12728	0.01	-0.01
6	4	13122	0.01	0.00
7	2	15852	-0.01	-0.01
8	2	16191	-0.01	0.01
9	2	18320	0.25	0.00
10	2	18390	0.00	0.00
11	2	20441	13.24	0.00
12	4	21282	0.07	0.07
13	4	21544	0.08	-0.08
14	2	21784	-0.08	0.06

15	2	21857	0.02	-0.03
16	2	22007	-1.49	1.38
17	2	22036	-1.59	-1.46
18	2	22594	0.00	0.00
19	4	23238	0.00	0.00
20	2	24592	0.00	0.00
21	2	24802	0.00	0.00
22	2	27227	0.00	0.00
23	2	27260	-0.01	0.00
24	2	28909	-0.31	0.29
25	2	29107	-0.30	-0.29
26	2	29632	-0.06	0.06
27	2	29852	-0.02	-0.02
28	2	30876	-0.02	0.01
29	2	31052	-0.03	-0.04
30	2	31725	1.44	0.00
31	2	32228	0.01	0.00
32	2	32268	0.01	0.00
33	2	33198	0.00	0.00
34	2	33436	-0.03	-0.03
35	2	33489	-0.03	0.03
36	2	34636	-0.55	-0.55
37	2	34969	-0.57	0.57
38	2	42821	0.00	0.00
39	2	42827	0.00	0.00
40	2	43560	-0.19	-0.18
41	2	43627	-0.19	0.18
42	2	43971	-0.01	0.00
43	2	44054	0.00	0.00
44	2	44316	0.00	0.00
45	2	64124	0.00	0.00
46	2	64129	0.00	0.00
47	2	64653	0.00	0.00
48	2	64708	0.00	0.00
49	2	65654	0.21	0.00

References

1. M. Dey, S. Dutta, B. Sarma, R. C. Deka and N. Gogoi, *Chem. Commun.*, 2016, **52**, 753-756.
2. L. Chen, S.-Y. Chen, Y.-C. Sun, Y.-M. Guo, L. Yu, X.-T. Chen, Z. Wang, Z. Ouyang, Y. Song and Z.-L. Xue, *Dalton Trans.*, 2015, **44**, 11482-11490.